Contribution from the Istituto per lo Studio della Stereochimica ed Energetica dei Composti di Coordinazione, CNR, Via J. Nardi 39, 50132 Firenze, Italy, Dipartimento di Chimica, Università di Siena, Via Pian dei Mantellini, 53100 Siena, Italy, and Dipartimento di Chimica, Università di Firenze, 50100 Firenze, Italy

Electrochemistry as a Diagnostic Tool To Discriminate between Classical M-$(H)_2$ and Nonclassical M-(H_2) Structures within a Family of Dihydride and Dihydrogen Metal Complexes

Claudio Bianchini,*[†] Franco Laschi,[‡] Maurizio Peruzzini,[†] Francesca M. Ottaviani,[§] Alberto Vacca,[†] and Piero Zanello[‡]

Received April 6, 1990

The redox properties of a family of dihydride and dihydrogen complexes of iron, cobalt, rhodium, and iridium have been studied in detail and compared with those of the corresponding monohydrido derivatives. All of the complexes contain as stabilizing coligands either $P(CH_2CH_2PPh_2)_3$ (PP_3) or $N(CH_2CH_2PPh_2)_3$ (NP_3). The novel dihydride $[(PP_3)Fe(H)_2]$ and its isotopomers $[(PP_3)Fe(H)(D)]$ and $[(PP_3)Fe(D)_2]$ have been fully characterized by IR and ^1H and ^{31}P NMR techniques. The complexes $[(PP_3)Co(H_2)]PF_6$ and $[(PP_3)Rh(H_2)]BF_4$, which exhibit the nonclassical dihydrogen structure, undergo in tetrahydrofuran irreversible one-electron oxidation. As a result, the deprotonation of the H_2 ligand occurs and the starting η^2-H_2 compounds are converted to the corresponding monohydrides $[(PP_3)MH]^+$ (M = Co, Rh). In contrast, the classical dihydrides $[(L)Ir(H)_2]BPh_4$ (L = PP_3, NP_3) and $[(NP_3)Rh(H)_2]BPh_4$ show no redox activity within the potential window of tetrahydrofuran. The dihydride $[(PP_3)Fe(H)_2]$ can be oxidized to give the unstable species $[(PP_3)Fe(H)_2]^+$ and $[(PP_3)Fe(H)_2]^{2+}$, but no deprotonation reaction occurs. The *cis*-(hydride)(dihydrogen) complex $[(PP_3)Fe(H)(H_2)]BPh_4$ undergoes one-electron reduction in tetrahydrofuran to give the neutral dihydride. Rare examples of paramagnetic monohydrides of cobalt(II), rhodium(II), iron(I), and iron(II) have been synthesized chemically or electrochemically and characterized by X-band ESR spectroscopy.

The bonding model for η^2-H_2 coordination, occurring through cooperative σ-donation/π-back-donation effects, bears some resemblance to metal-olefin π-bonding.[1-3] However, only for H_2 can the interaction between a suitable filled metal π orbital and σ^*(H-H) be strong enough to promote the cleavage of the molecule. When this occurs, and in most instances it does, the formal oxidation state of the metal is increased by 2 units and a metal dihydride forms. Accordingly, provided a change in the oxidation state of the metal occurs on going from M-(H_2) to M-$(H)_2$, a study of the redox properties of the complexes could be extremely useful in elucidating the structure.

To explore such a possiblity, we began a detailed study on the redox properties of several known and novel complexes of group VIII metals for which either the classical or the nonclassical structure have been determined. The following compounds have been investigated: $[(PP_3)Co(H_2)]PF_6$ (**1**),[2j] $[(PP_3)Rh(H)_2]BF_4$ (**2**),[4] $[(PP_3)Ir(H)_2]BPh_4$ (**13**),[5] $[(NP_3)Rh(H)_2]BPh_4$ (**14**),[6] $[(NP_3)Ir(H)_2]BPh_4$ (**15**),[6] $[(PP_3)Fe(H)_2]$ (**3**), and $[(PP_3)Fe(H)(H_2)]BPh_4$ (**4**)[2i] [PP_3 = $P(CH_2CH_2PPh_2)_3$; NP_3 = $N(CH_2CH_2PPh_2)_3$]. The redox properties of the above compounds have been compared and contrasted with those of the monohydrido complexes $[(PP_3)CoH]$ (**6**),[7a] $[(NP_3)CoH]$ (**9**),[7b] $[(PP_3)RhH]$ (**12**),[6] and $[(PP_3)FeH]BF_4$ (**5**). Interestingly, we have found that, for the η^2-H_2 ligands supported by d^8 L_4M fragments, the one-electron oxidation results in a deprotonation reaction and consequent conversion of the starting complexes to the corresponding monohydrides $[(PP_3)MH]^+$ (M = Co, Rh).

Results and Discussion

Sixteen-Electron fragments of cobalt, rhodium, and iridium with the tripodal polyphosphine ligands PP_3 and NP_3 can be generated in situ by either protonation of M(I) σ-methyl complexes or alkylation of M(I) monohydrido complexes.[2j,4-6] Except for the trigonal-pyramidal, paramagnetic cation $[(NP_3)Co]^+$, which is stable and isolable as its BF_4^- salt,[8] all of the other systems react with molecular hydrogen, affording either classical *cis*-dihydrides or nonclassical η^2-H_2 complexes (Scheme I).[2j,4-6]

Synthesis and Characterization of the Novel Complexes $[(PP_3)Fe(H)_2]$ and $[(PP_3)FeH]BF_4$. Stirring an equimolar mixture of anhydrous $FeCl_2$ and PP_3 in THF with an excess of $NaBH_4$ results in the formation of an orange solution from which diamagnetic crystals of $[(PP_3)Fe(H)_2]$ (**3**) are precipitated by addition of ethanol. Compound **3** is fairly stable in the solid state and in deareated solutions in which it behaves as a nonelectrolyte. The IR spectrum contains ν(Fe-H) at 1850 (s) and 1740 (s) cm^{-1}.

[†] ISSECC, CNR.
[‡] University of Siena.
[§] University of Firenze.

(1) For comprehensive reviews on molecular hydrogen complexes, see: (a) Kubas, G. J. *Acc. Chem. Res.* **1988**, *21*, 120. (b) Kubas, G. J. *Comments Inorg. Chem.* **1988**, *7*, 17. (c) Henderson, R. A. *Transition Met. Chem. (N.Y.)* **1988**, *13*, 474. (d) Crabtree, R. H.; Hamilton, D. G. *Adv. Organomet. Chem.* **1988**, *28*, 299.

(2) Since the reviews quoted in ref 1, several additional dihydrogen complexes have been reported: (a) Airliguie, T.; Chaudret, B.; Morris, R. H.; Sella, A. *Inorg. Chem.* **1988**, *27*, 598. (b) Fontaine, X. L. R.; Fowles, E. H.; Shaw, B. L. *J. Chem. Soc., Chem. Commun.* **1988**, 482. (c) Baker, M. V.; Field, L. D.; Young, D. J. *J. Chem. Soc., Chem. Commun.* **1988**, 546. (d) Bautista, M. T.; Earl, K. A.; Morris, R. H. *Inorg. Chem.* **1988**, *27*, 1124. (e) Bautista, M. T.; Earl, K. A.; Maltby, P. A.; Morris, R. H. *J. Am. Chem. Soc.* **1988**, *110*, 4056. (f) Hampton, C.; Dekleva, T. W.; James, B. R.; Cullen, W. R. *Inorg. Chim. Acta* **1988**, *145*, 165. (g) Hampton, C.; Cullen, W. R.; James, B. R. *J. Am. Chem. Soc.* **1988**, *110*, 6918. (h) Cotton, F. A.; Luck, R. L. *J. Chem. Soc., Chem. Commun.* **1988**, 1277. (i) Bianchini, C.; Peruzzini, M.; Zanobini, F. *J. Organomet. Chem.* **1988**, *354*, C19. (j) Bianchini, C.; Mealli, C.; Meli, A.; Peruzzini, M.; Zanobini, F. *J. Am. Chem. Soc.* **1988**, *110*, 8725. (k) Airliguie, T.; Chaudret, B.; Morris, R. H. *Polyhedron* **1988**, *7*, 2031. (l) Esteruelas, M. A.; Sola, E.; Oro, L. A.; Meyer, U.; Werner, H. *Angew. Chem., Int. Ed. Engl.* **1988**, *27*, 1563. (m) Jia, G.; Meek, D. W. *J. Am. Chem. Soc.* **1989**, *111*, 757. (n) Airliguie, T.; Chaudret, B. *J. Chem. Soc., Chem. Commun.* **1989**, 155. (o) Antoniutti, S.; Albertin, G.; Amendola, P.; Bordignon, E. *J. Chem. Soc., Chem. Commun.* **1989**, 229. (p) Antoniutti, S.; Albertin, G.; Bordignon, E. *J. Am. Chem. Soc.* **1989**, *111*, 2072. (q) Chinn, M. S.; Heinekey, D. M.; Payne, N. G.; Sofield, C. D. *Organometallics* **1989**, *8*, 1824. (r) Cotton, F. A.; Luck, R. L. *Inorg. Chem.* **1989**, *28*, 2181. (s) Johnson, T. J.; Huffmann, J. C.; Caulton, K. G.; Jackson, S. A.; Eisenstein, O. *Organometallics* **1989**, *8*, 2073. (t) Nolan, S. P.; Marks, T. J. *J. Am. Chem. Soc.* **1989**, *111*, 8538. (u) Joshi, A. M.; James, B. R. *J. Chem. Soc., Chem. Commun.* **1989**, 1785. (v) Mediati, M.; Tachibana, G. N.; Jensen, C. M. *Inorg. Chem.* **1990**, *29*, 3. (w) Collman, J. P.; Wagenknecht, P. S.; Hembre, R. T.; Lewis, N. S. *J. Am. Chem. Soc.* **1990**, *112*, 1294.

(3) For theoretical studies on molecular hydrogen complexes, see: (a) Hay, P. J. *Chem. Phys. Lett.* **1984**, *103*, 466. (b) Saillard, J.-Y.; Hoffmann, R. *J. Am. Chem. Soc.* **1984**, *106*, 2006. (c) Jean, Y.; Eisenstein, O.; Volatron, F.; Maouche, B.; Sefta, F. *J. Am. Chem. Soc.* **1986**, *108*, 6587. (d) Hay, P. J. *J. Am. Chem. Soc.* **1987**, *109*, 705. (e) Burdett, J. K.; Phillips, J. R.; Pourian, M. R.; Poliakoff, M.; Turner, J. J.; Upmacis, R. K. *Inorg. Chem.* **1987**, *26*, 3054. (f) Volatron, F.; Jean, Y.; Lledós, A. *Nouv. J. Chem.* **1987**, *11*, 651. (g) Maseras, F.; Duran, M.; Lledós, A.; Bertran, J. *Inorg. Chem.* **1989**, *28*, 2984. (h) Pacchioni, G. *J. Am. Chem. Soc.* **1990**, *112*, 80.

(4) Bianchini, C.; Mealli, C.; Peruzzini, M.; Zanobini, F. *J. Am. Chem. Soc.* **1987**, *109*, 5548.

(5) Bianchini, C.; Peruzzini, M.; Zanobini, F. *J. Organomet. Chem.* **1987**, *326*, C79.

(6) Bianchini, C.; Masi, D.; Meli, A.; Peruzzini, M.; Zanobini, F. *J. Am. Chem. Soc.* **1988**, *110*, 6411.

(7) (a) Ghilardi, C. A.; Midollini, S.; Sacconi, L. *Inorg. Chem.* **1975**, *14*, 1790. (b) Sacconi, L.; Ghilardi, C. A.; Mealli, C.; Zanobini, F. *Inorg. Chem.* **1975**, *14*, 1830.

0020-1669/90/1329-3394$02.50/0

Scheme I

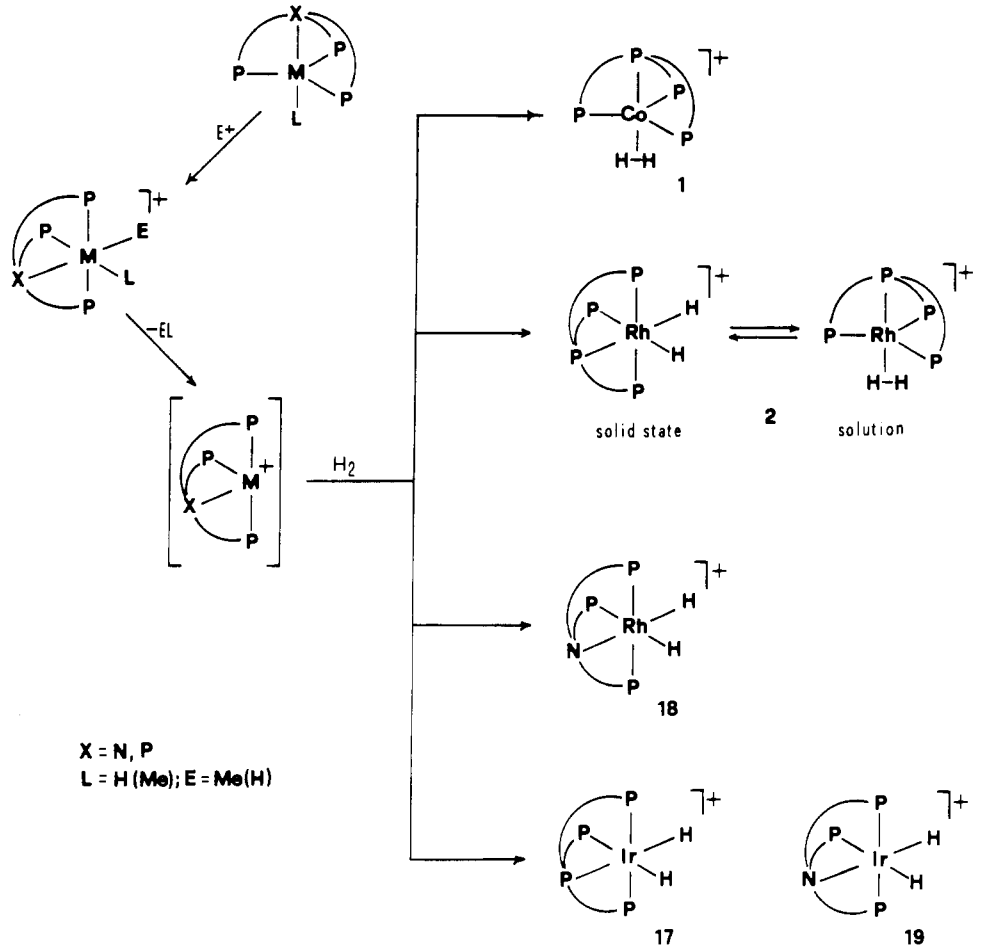

Such an assignment is supported by the IR spectrum of the perdeuterated isotopomer [(PP$_3$)Fe(D)$_2$] (**3**-d_2), in which the two bands are shifted to lower energy by ca. 500 cm^{-1} [ν(Fe-D) at 1338 and 1260 cm^{-1}]. The ^{31}P{^{1}H} NMR spectrum (THF-d_8, 121.42 MHz) consists of an AM$_3$ spin system over the temperature range 303–193 K. The chemical shift of the bridgehead phosphorus falls largely downfield [δ(P$_A$) 182.57 ppm at 293 K, J(P$_A$P$_M$) = 12.1 Hz], as expected for its involvement in three five-membered rings.[6,9] A doublet centered at 102.13 ppm (3 P) is readily assigned to the three equivalent terminal phosphorus of PP$_3$. Decreasing the temperature broadens the two resonances, until at 173 K any fine structure is lost and the spectrum consists of two broad signals in a 1:3 intensity ratio [$w_{1/2}$(P$_A$) = 66 Hz; $w_{1/2}$(P$_M$) = 62 Hz]. The AM$_3$ spin system is typical of trigonal-bipyramidal (TBP) metal complexes of PP$_3$ in which the coligand trans to the bridgehead phosphorus does not destroy the C_{3v} symmetry.[6,10] In general, however, the ^{31}P NMR signals of the PP$_3$ ligand in such compounds do not exhibit temperature-dependent line widths as occurs for **3**. Accordingly, the spectrum could be interpreted in a manner essentially similar to that used for the rhodium analogue **2**, i.e. a temperature-dependent interconversion between TBP η^2-H$_2$ and octahedral (OCT) *cis*-(H)$_2$ tautomers, the only difference being a lower temperature at which the limiting dihydride structure begins to form (<183 K). A second, reasonable interpretation of the spectrum is to think of a fluxional *cis*-dihydride OCT complex molecule in which the hydride ligands exchange very rapidly so as to make the three terminal phosphorus of PP$_3$ equivalent on the NMR time scale.

The ^{1}H NMR spectrum (toluene-d_8, 300 MHz) does not permit one to discriminate between the two models. A single resonance (2 H) is displayed in the hydride region over the temperature range 303–200 K (Figure 1). At room temperature, the signal appears as a broad quartet centered at −10.45 ppm. This multiplicity arises from a much larger coupling of the two hydrogen nuclei to the three terminal phosphorus atoms [J(HP$_{cis}$) = 42.0 Hz], as is clearly shown by ^{31}P-decoupling experiments. A calculated value of ca. 3 Hz is assigned to J(HP$_{trans}$) to account for the observed line width of the resonance ($w_{1/2}$ = 6.5 Hz). On a decrease in temperature, the reasonance broadens while slightly shifting to lower field and, finally, at 173 K collapses. Again, this behavior parallels that of the rhodium complex **2**, for which the coalescence point separating the η^2-H$_2$ and *cis*-(H)$_2$ tautomers was observed at 193 K.[4]

Analysis of the T_1 values for the hydride signal in the spectrum of **3** (toluene-d_8, 300 MHz, inversion-recovery method) over the temperature range 303–200 K shows that the relaxation time strongly depends on the temperature and goes through a minimum of 145 (±20) ms at 253 K. Such a value is too high for an η^2-ligand but falls in the proper range for a hydrido complex of iron(II).[2d,e,o,p,11] Conclusive evidence for a *cis*-dihydride structure of **3** is provided by H/D exchange experiments. In particular, treatment of an equimolar mixture of anhydrous FeCl$_2$ and PP$_3$ in THF with an excess of NaBD$_4$, followed by addition of CH$_3$CH$_2$OD results in the precipitation of a mixture of **3**-d_2 [55 (2)%)], **3** [20 (2)%], and [(PP$_3$)Fe(H)(D)] (**3**-d_1) [25 (2)%] [the percentage of each compound was determined both by ^{31}P{H} and ^{1}H NMR integration and computer simulation of the spectra (see

(8) Sacconi, L.; Orlandini, A.; Midollini, S. *Inorg. Chem.* **1974**, *13*, 2850.
(9) Garrou, P. E. *Chem. Rev.* **1981**, *81*, 229.
(10) (a) Hohman, W. H.; Kountz, D. J.; Meek, D. W. *Inorg. Chem.* **1986**, *25*, 616. (b) Gambaro, J. J.; Hohman, W. H.; Meek, D. W. *Inorg. Chem.* **1989**, *28*, 4154. (c) Bianchini, C.; Masi, D.; Meli, A.; Peruzzini, M.; Ramierz, J. A.; Vacca, A.; Zanobini, F. *Organometallics* **1989**, *8*, 2179. (d) Bianchini, C.; Laschi, F.; Ottaviani, M. F.; Peruzzini, M.; Zanello, P.; Zanobini, F. *Organometallics* **1989**, *8*, 893.
(11) (a) Bautista, M. T.; Earl, K. A.; Morris, R. H.; Sella, A. *J. Am. Chem. Soc.* **1987**, *109*, 3780. (b) Bautista, M. T.; Earl, K. A.; Maltby, P. A.; Morris, R. H.; Schweitzer, C. T.; Sella, A. *J. Am. Chem. Soc.* **1988**, *110*, 7031. (c) Hamilton, D. G.; Crabtree, R. H. *J. Am. Chem. Soc.* **1988**, *110*, 4126.

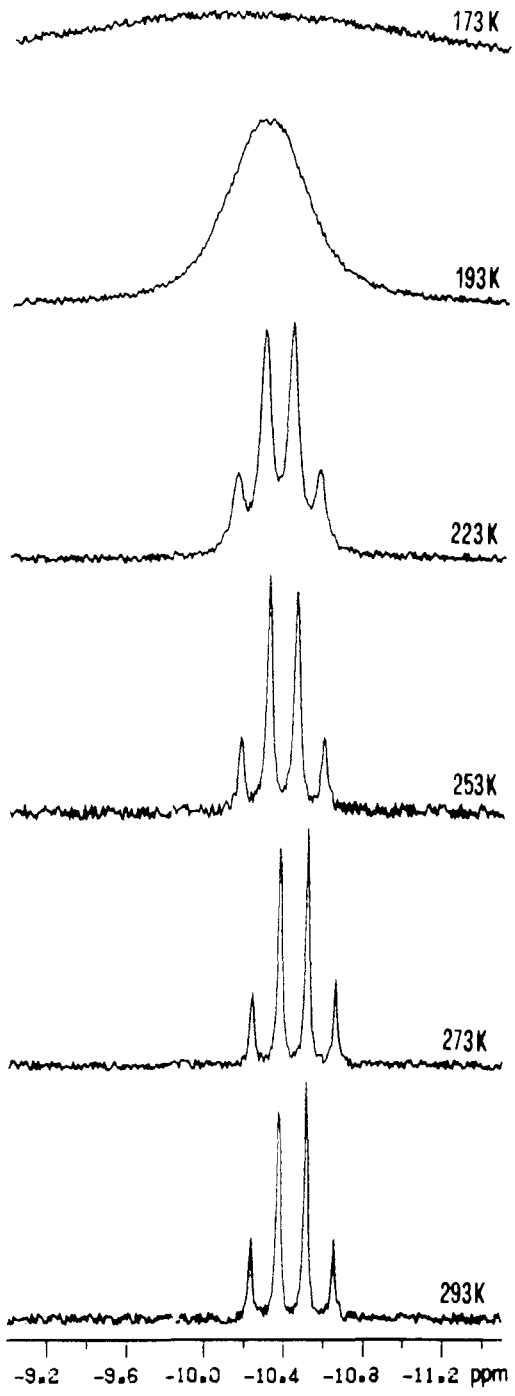

Figure 1. Variable-temperature ^1H NMR spectra of **3** in the hydride region (toluene-d_8, 300 MHz, Me_4Si reference).

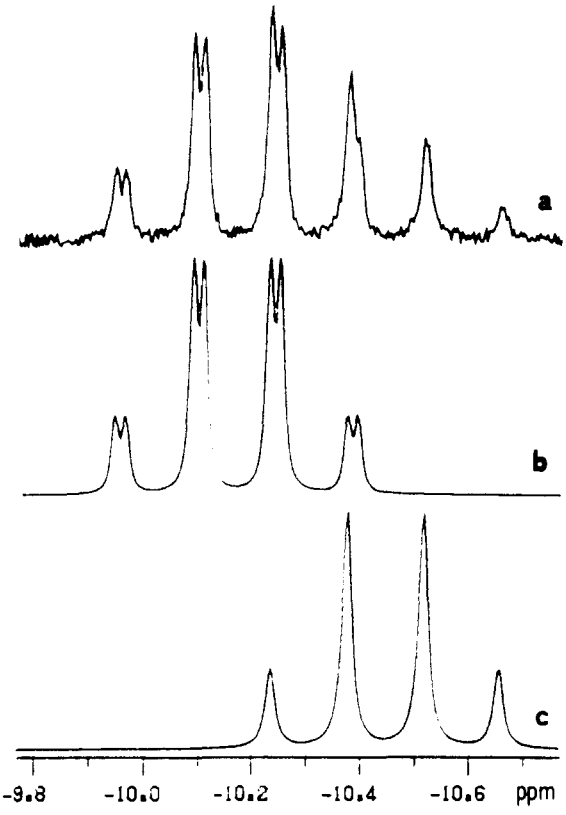

Figure 2. ^1H NMR spectra of a mixture of **3** and **3**-d_1 in the hydride region (toluene-d_8, 300 MHz, 293 K, Me_4Si reference): (a) experimental spectrum; (b) computed contribution of **3**-d_1; (c) computed contribution of **3**.

Scheme II

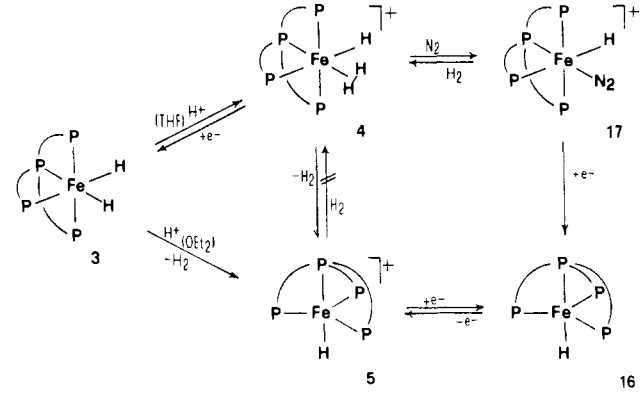

below); standard deviations are given in parentheses]. A quite similar product distribution is obtained by reaction of **3** in THF with an excess of $NaBD_4$. As expected, the ^1H NMR spectrum of the precedent isotopomeric mixture (toluene-d_8, 293 K, 300 Mz) contains in the hydride region a second resonance at −10.17 ppm in addition to the quartet of **3** (Figure 2). The new multiplet that appears as a quartet of doublets is assigned to the hydride ligand in the deuteride hydride **3**-d_1. The qd pattern is originated by coupling to the magnetically equivalent, terminal phosphorus nuclei [$J(HP_{cis})$ = 43.0 Hz] and to the bridgehead phosphorus [$J(HP_{trans})$ = 5.8 Hz]. A calculated value of ca. 1 Hz is assigned to J(HD), which is typical of *cis*-(deuteride)(hydride) complexes with no H–D bonding interaction.[12] The larger $J(HP_{trans})$ value in **3**-d_1 as compared to **3** may be due to a slower H/D vs H/H exchange. Interestingly, upon deuteration there is an isotope effect on the chemical shift of the hydride resonance of ca. 0.25 ppm. This is a remarkable effect and could be an example of IPR (isotopic perturbation of the resonance position).[13]

On the basis of all of these data, a structure can be assigned to **3** where iron is octahedrally coordinated by the four phosphorus donors of PP_3 and by two mutually cis hydride ligands (Scheme II).

The $^{31}P\{^1H\}$ NMR spectrum of the mixture of **3** and its deuterated isotopomers (toluene-d_8, 293 K, 121.42 MHz) consists of three low-field quartets approximately in a 1:2:1 ratio and of a higher field multiplet in the region of the terminal phosphorus of PP_3. The quartets are readily assigned to the bridgehead phosphorus of the three isotopomers, respectively, the assignment being done with the procedure described below. The chemical shifts and coupling constants are as follows: **3**, $\delta(P_b)$ = 182.57, $J(P_bP_t)$ = 12.1 Hz; **3**-d_1, $\delta(P_b)$ = 182.40, $J(P_bP_t)$ = 11.9 Hz; **3**-d_2, $\delta(P_b)$ = 182.50, $J(P_bP_t)$ = 12.1 Hz (b = bridgehead; t = terminal).

(12) Moore, D. S.; Robinson, S. D. *Chem. Soc. Rev.* **1983**, *12*, 415.

(13) Luo, X.-L.; Crabtree, R. H. *Inorg. Chem.* **1989**, *28*, 3775 and references therein.

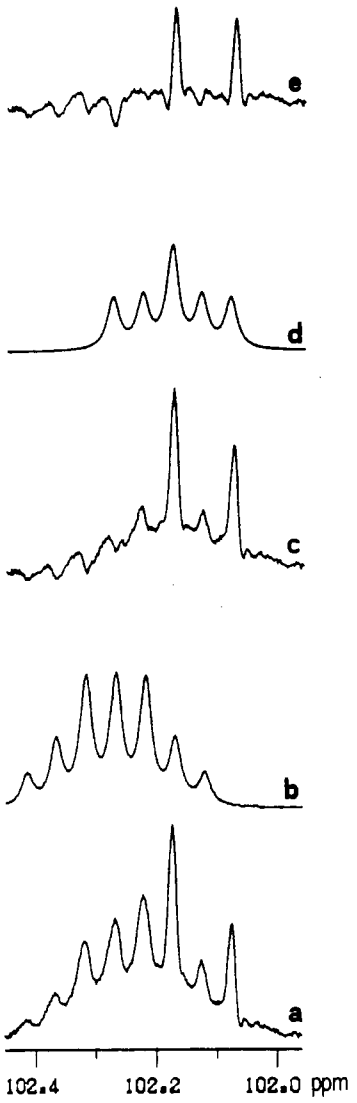

Figure 3. (a) Experimental $^{31}P\{^1H\}$ NMR spectrum in the region of the terminal phosphorus atoms of PP_3 of a mixture of **3**, **3**-d_1, and **3**-d_2 (toluene-d_8, 121.42 MHz, 293 K, 85% H_3PO_4 reference). (b) Computed spectrum of the perdeuterated complex **3**-d_2. (c) Spectrum resulting from the subtraction of the spectrum shown in part b from the spectrum shown in part a. (d) Computed spectrum of the hydride deuteride complex **3**-d_1. (e) Spectrum resulting from the subtraction of the spectrum shown in part d from the spectrum shown in part c.

The high-field multiplet shown in Figure 3a has been analyzed through a *striptease* technique using a modified version of the computer package DAVINS.[14] The three terminal phosphorus atoms of PP_3 in the perdeuterated isotopomer **3**-d_2 are expected to constitute the M_3 portion of an AM_3X_2 system in which the nuclei A, M, and X exhibit I values of $^1/_2$, $^1/_2$, and 1, respectively. In light of the $^{31}P\{^1H\}$ and ^1H NMR spectra of **3** and **3**-d_1 (^1H), a septuplet structure with a 1:2:4:4:4:2:1 intensity ratio has been calculated for the terminal phosphorus, by using the following parameters: $\delta(P_A)$ 102.27 ppm, $J(P_bP_t)$ = 12.0 Hz, $J(P_bD)$ = 6.0 Hz, $J(P_tD)$ = 0 Hz (Figure 3b). Subtraction of the computed septuplet relative to the perdeuterated isotopomer **3**-d_2 from the experimental spectrum still results in a complicated multiplet (Figure 3c). A quintet with a 1:1:2:1:1 intensity ratio (M_3 portion of an AM_3X spin system with A = P, M = P, and X = D) is calculated for the three terminal phosphorus atoms of **3**-d_1, by using the following parameters: $J(P_bP_t)$ = 11.9 Hz, $J(P_bD)$ = 5.9 Hz (Figure 3d). When the calculated quintet centered at 102.18 ppm is subtracted from the spectrum shown in Figure 3c, only a doublet remains, which just corresponds to the experimental resonance of the three terminal phosphorus nuclei in the dihydride **3** (Figure 3e). The percentages of each compound used to strip or, reversibly, build up the experimental spectrum shown in Figure 3a are 55 (2)% (**3**-d_2), 25 (2)% (**3**-d_1), and 20 (2)% (**3**), which is in good accord with the product composition obtained by NMR integration of the bridgehead phosphorus signals.

Pure perdeuterated compound **3**-d_2 as analyzed by means of IR spectroscopy can be obtained by repeated treatment of the mixture of the three isotopomers in anhydrous THF with an excess of $NaBD_4$. Its dissolution in solvents such as toluene, benzene, or THF results in the formation of equilibrium concentrations of the two deuterated isotopomers, the product distribution depending on the grade of hydration of the solvents. As a matter of fact, addition of water causes the quantitative conversion to the dihydride **3**.[15]

The chemistry of **3** is fully consistent with the classical *cis*-dihydride structure. The compound is not deprotonated by strong bases whereas it reacts with protic acids in a manner that depends on the solvent (Scheme II). In particular, protonation by $HBF_4 \cdot Et_2O$ in THF under argon occurs at the metal to give after metathetical reaction with $NaBPh_4$, the known *cis*-(hydride)(η^2-dihydrogen) complex $[(PP_3)Fe(H)(H_2)]BPh_4$ (**4**).[2i] In contrast, **3** suspended in ethyl ether reacts with tetrafluoroboric acid, converting to violet microcrystals of the novel Fe(II) hydride $[(PP_3)FeH]BF_4$ (**5**). Alternatively, **5** can be obtained by bubbling argon throughout a solution of **4** in THF followed by EtOH addition. In contrast, **5** dissolved in THF does not transform into **4** by treatment with H_2. This is ascribed to the high-spin electronic configuration of **5**, which is paramagnetic with a magnetic moment corresponding to two unpaired spins (μ_{eff} = 3.05 μ_B). It is fairly stable in the solid state and in deaerated solutions, in which it behaves as a 1:1 electrolyte. The IR spectrum shows no band that can be assigned to ν(Fe-H). This is quite common for paramagnetic hydrido complexes stabilized by tripodal ligands.[16] Conclusive evidence of the presence of a terminal hydride ligand in **5** is provided by the reaction with CCl_4, producing $CHCl_3$ and the known[17] complex $[(PP_3)FeCl]BPh_4$. The diffuse-reflectance spectrum has three bands at 8400, 10 400 (sh), and 18 600 cm^{-1}. Both the magnetic moment and the UV-visible spectrum are diagnostic of TBP coordination around the Fe(II) metal center (Scheme II).[18] The TBP structure is supported by the X-band ESR spectrum in THF, which consists of a broad unresolved signal even for the frozen solution with $\langle g \rangle$ = 2.028 (ΔH_{tot} = 300 G at 300 K). The absence of hyperfine structure is quite common for systems having two unpaired electrons,[19] while the $\langle g \rangle$ parameter falls in the proper range for TBP iron(II) complexes stabilized by the PP_3 ligand, such as $[(PP_3)Fe(C{\equiv}CR)]BPh_4$ (R = alkyl, aryl).[20]

Interestingly, **5** does not convert to the parent dihydride **3** by reaction with an excess of $NaBH_4$ in THF, most likely because of its triplet ground state.

Electrochemical Studies

$[(PP_3)Co(\eta^2\text{-}H_2)]^+$ vs $[(PP_3)CoH]$. Figure 4 compares the redox propensity of **1** (a) with that exhibited by $[(PP_3)CoH]^+$[7a] (**6**) (b) in THF solution. It is evident that the dihydrogen complex undergoes oxidation at peak A (E_p = +0.45 V) showing no directly associated rereduction peak in the reverse scan, even at the scan rate of 10 V s^{-1}. Such an irreversible process, which proves coulometrically to involve one-electron/molecule, generates the

(14) (a) Stephenson, D. S.; Binsch, G. *J. Magn. Reson.* **1980**, *37*, 395. (b) Stephenson, D. S.; Binsch, G. *J. Magn. Reson.* **1980**, *37*, 409.

(15) A reviewer has suggested that the proton-exchange reaction in wet solvent could proceed via protonation to give **4**, followed by deprotonation of the acidic η^2-H_2 ligand.

(16) Bianchini, C.; Masi, D.; Mealli, C.; Meli, A.; Sabat, M. *Gazz. Chim. Ital.* **1986**, *116*, 201.

(17) Stoppioni, P.; Mani, F.; Sacconi, L. *Inorg. Chim. Acta* **1974**, *11*, 227.

(18) (a) Morassi, R.; Bertini, I.; Sacconi, L. *Coord. Chem. Rev.* **1973**, *11*, 343. (b) Sacconi, L.; Di Vaira, M. *Inorg. Chem.* **1978**, *17*, 810. (c) Di Vaira, M.; Midollini, S.; Sacconi, L. *Inorg. Chim.* **1977**, *16*, 1518.

(19) Bencini, S.; Gatteschi, D. *Transition Met. Chem. (N.Y.)* **1982**, *8*, 201.

(20) Bianchini, C.; Meli, A.; Peruzzini, M.; Vizza, F.; Zanobini, F.; Frediani, P. *Organometallics* **1989**, *8*, 2080.

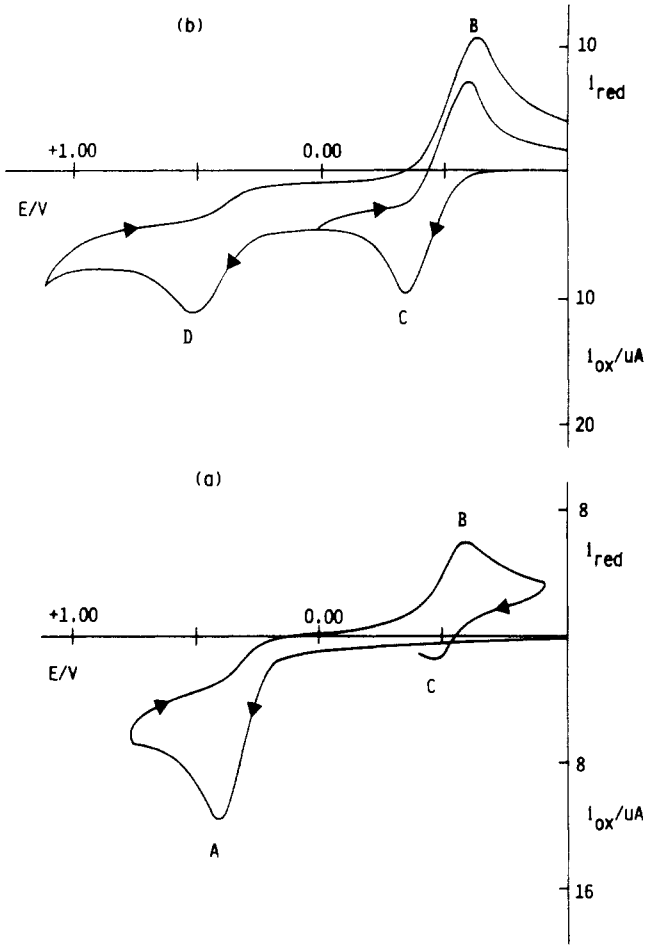

Figure 4. Cyclic voltammograms of deaerated THF solutions containing $[NBu_4]ClO_4$ (0.1 mol dm^{-3}) recorded at a platinum electrode: (a) complex **1** (1.40×10^{-3} mol dm^{-3}); (b) complex **6** (1.48×10^{-3} mol dm^{-3}). Scan rate = 0.2 V s^{-1}.

oxidized form of **6**, namely $[(PP_3)CoH]^+$. In fact, **6** undergoes, through a quasireversible step, a chemically reversible one-electron oxidation to form $[(PP_3)CoH]^+$ at $E^{o\prime} = -0.48$ V (peak system C/B in Figure 4b), followed by a further irreversible anodic step D at $E_p = +0.49$ V. Accordingly, we reasonably conclude that, upon one-electron oxidation, **1** converts to $[(PP_3)CoH]^+$ while a proton is liberated.

$$[(PP_3)Co(H_2)]^+ \xrightarrow[-H^+]{-e^-} [(PP_3)CoH]^+$$

Further support of this reaction pathway is provided by ESR spectroscopy. In fact, the X-band ESR spectrum recorded on the solution of **1** after exhaustive one-electron oxidation in THF is fully coincident with that of the known Co(II) complex $[(PP_3)CoH]BF_4$ (**7**), synthesized by reaction of an equimolar mixture of $Co(BF_4)_2 \cdot 6H_2O$, PP_3, and $NaBH_4$.[7a] Compound **7** is paramagnetic, with a magnetic moment corresponding to one unpaired spin ($\mu_{eff} = 2.01\ \mu_B$), and can be prepared also by treatment of **6** in THF with 1 equiv of $[(C_5H_5)_2Fe]PF_6$, followed by metathetical reaction with a large excess of $[NBu_4]BF_4$. Alternatively, the perchlorate salt $[(PP_3)CoH]ClO_4$ (**8**) is synthesized by exhaustive one-electron macroelectrolysis of a solution of **1** ($[NBu_4]ClO_4$ as supporting electrolyte).

Valuable information on the solution structure of **7** is provided by ESR spectroscopy. The X-band ESR spectrum in THF at 320 K consists of a broad, unresolved signal centered at $\langle g \rangle = 2.107$ ($\Delta H_{tot} = 153$ G) (Figure 5a). On a decrease in temperature, the spectrum resolves, showing the presence of two paramagnetic contributions. At 250 K, the two species exhibit $\langle g \rangle$ values of 2.130 and 2.081 (Figure 5b). Indeed, the spectrum in THF glass at 100 K (Figure 5c) has been nicely computed as the sum of two contributions with $S = {}^1/_2$ in a 3:2 ratio (dashed line) with $g_1 =$ 2.200 ($A_1 = 56.5$ G), $g_2 = 2.190$ ($A_2 = 13.5$ G), $g_3 = 2.120$ ($A_3 = 16.6$ G) and $g_1 = 2.090$ ($A_1 = 25.0$ G), $g_2 = 2.040$ ($A_2 = 10.0$ G), $g_3 = 1.990$ ($A_3 = 68.0$ G), respectively. The hyperfine structure is attributed to coupling of the unpaired electron to the ^{59}Co nucleus.[21] The much stronger coupling of the electron to cobalt rather than to phosphorus has numerous precedents for tripodal polyphosphine Co(II) complexes.[21] The magnetic parameters are consistent with a distorted TBP geometry around Co(II) for the major species and with a square-pyramidal (SQ) structure for the minor species.[19,21] A fast interconversion between TBP and SQ geometries has been previously observed for five-coordinate Co(II) complexes with the tripodal phosphine $MeC(CH_2PPh_2)_3$ (triphos).[21a,b]

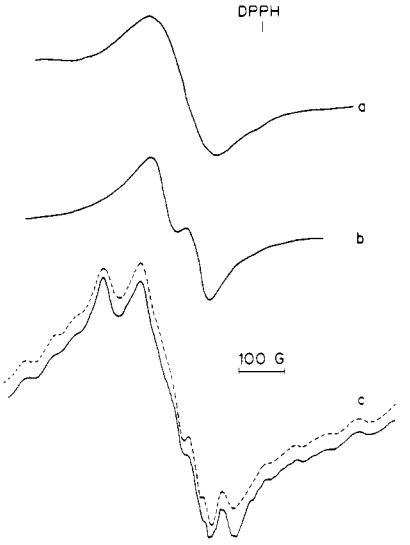

Figure 5. X-Band ESR spectra of **7** in THF: (a) $T = 320$ K; (b) $T = 250$ K; (c) $T = 100$ K. Dashed line: computed spectrum at 100 K.

Scheme III

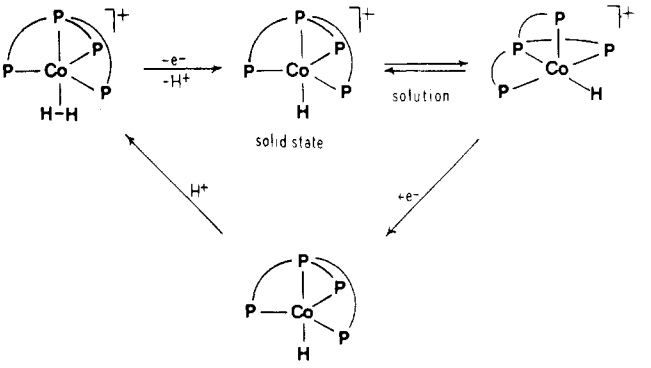

The chemical and electrochemical transformations involving the $[(PP_3)Co(H_2)]^+/[(PP_3)CoH]$ system are appropriately summarized in Scheme III.

No reduction process associated with **1** occurs within the potential window of THF.

The quasireversibility of the electrochemical step $[(PP_3)CoH]/[(PP_3)CoH]^+$ deserves some comments. It is well-known that the rate of the heterogeneous electron transfer between the electrode and a metal complex is largely determined by the occurrence of significant structural rearrangements within the complex framework. Such rearrangements raise the activation barrier to the charge transfer and slow down the rate of the redox

(21) (a) Bianchini, C.; Masi, D.; Mealli, C.; Meli, A.; Martini, G.; Laschi, F.; Zanello, P. *Inorg. Chem.* **1987**, *26*, 3683. (b) Bianchini, C.; Meli, A.; Laschi, F.; Vizza, F.; Zanello, P. *Inorg. Chem.* **1989**, *28*, 227. (c) Casagrande, L. V.; Chen, T.; Rieger, P. H.; Robinson, B. H.; Simpson, J.; Visco, S. J. *Inorg. Chem.* **1984**, *23*, 2019. (d) Nishida, Y.; Kida, S. *Bull. Chem. Soc. Jpn.* **1975**, *48*, 1045. (e) Nishida, Y.; Shimohori, H. *Bull. Chem. Soc. Jpn.* **1973**, *46*, 2406. (f) Stelzer, O.; Sheldrick, W. S.; Subramanian, J. *J. Chem. Soc., Dalton Trans.* **1977**, 966.

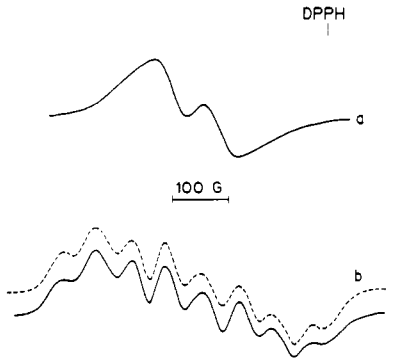

Figure 6. X-Band ESR spectra of **11** in THF: (a) T = 300 K; (b) T = 100 K. Dashed line: computed spectrum at 100 K.

change.[22] This is consistent with the significant geometrical reorganization of the complex upon one-electron oxidation and, in particular, with the presence of two isomeric forms of **7** in solution. On the other hand, the crystal structures of the two redox congeners **6** and **7** are known.[23,24] Both compounds adopt TBP geometries with the three phosphorus atoms in the equatorial plane and the bridgehead phosphorus and the hydride ligand in the axial positions. However, while the structure of **6** is quite regular, that of **7** is significantly distorted. In this respect, it is worth noticing that a distortion of the coordination polyhedron on going from **6** to **7** was expected because of the Jahn–Teller effect due to the presence one electron in an e orbital of a 3-fold symmetry system.[25] The isolation of a single isomer of **7** in the solid state was likely due to the crystallization process.

Protonation of the NP_3 analogue of **6**, namely $[(NP_3)CoH]$ (**9**), with tetrafluoroboric acid in THF does not result in the formation of a stable η^2-H_2 adduct. In fact, the system evolves H_2, and the paramagnetic, trigonal-pyramidal complex $[(NP_3)Co]BF_4$ (**10**) forms (μ_{eff} = 3.11 μ_B).[8] However, the redox properties of the cobalt monohydrido complex are quite similar to those of the PP_3 analogue **6**. As a matter of fact, **9** undergoes in THF a chemically reversible one-electron removal at $E^{\circ\prime}$ = −0.67 V, followed by a second irreversible step at E_p = +0.49 V.

The novel paramagnetic hydride $[(NP_3)CoH]ClO_4$ (**11**) can be prepared by exhaustive one-electron anodic macroelectrolysis of a THF solution of **9** and recrystallized from THF/*n*-heptane [IR 1850 (w) cm^{-1}, ν(Rh–H); μ_{eff} = 2.02 μ_B].

Like **7**, the NP_3 derivative **11** exists in THF solution as a mixture of two isomeric forms. These are observable by X-band ESR spectroscopy also at room temperature and exhibit $\langle g \rangle$ values of 2.180 and 2.120 (Figure 6a). In a similar way, the frozen-solution spectrum at 100 K (Figure 6b) is interpreted in terms of a superimposition of two contributions in ca. 2:1 ratio (dashed line: computed spectrum). On the basis of the Hamiltonian parameters, the predominant species is assigned a distorted TBP structure [g_1 = 2.165 ($A_{1Co} \cong$ 9 G), g_2 = 2.150 (A_{2Co} = 60 G), g_3 = 2.070 ($A_{3Co} \cong$ 9 G)]. In turn, the minor species adopts a SQ structure [g_1 = 2.250 ($A_{1Co} \cong$ 9 G), g_2 = 2.200 ($A_{2Co} \cong$ 9 G), g_3 = 2.147 (A_{3Co} = 62 G)].[19,21] From a perusal of these data, it is evident that replacement of phosphorus with nitrogen in the tripodal ligand significantly affects the magnetic parameters of the hydrides $[(L)CoH]^+$ (L = PP_3, NP_3), likely because of some changes in the secondary geometry.

$[(PP_3)Rh(\eta^2\text{-}H_2)]^+$ vs $[(PP_3)RhH]$. Figure 7a illustrates the electron-transfer ability of **2** in THF solution. The voltammogram was recorded immediately after the dissolution of the sample because of some decomposition (the compound slowly loses dihydrogen). Like the cobalt analogue **1**, the complex undergoes oxidation through an irreversible step at peak A (E_p = +0.73 V). The instability of **2** in solution prevents a precise coulometric

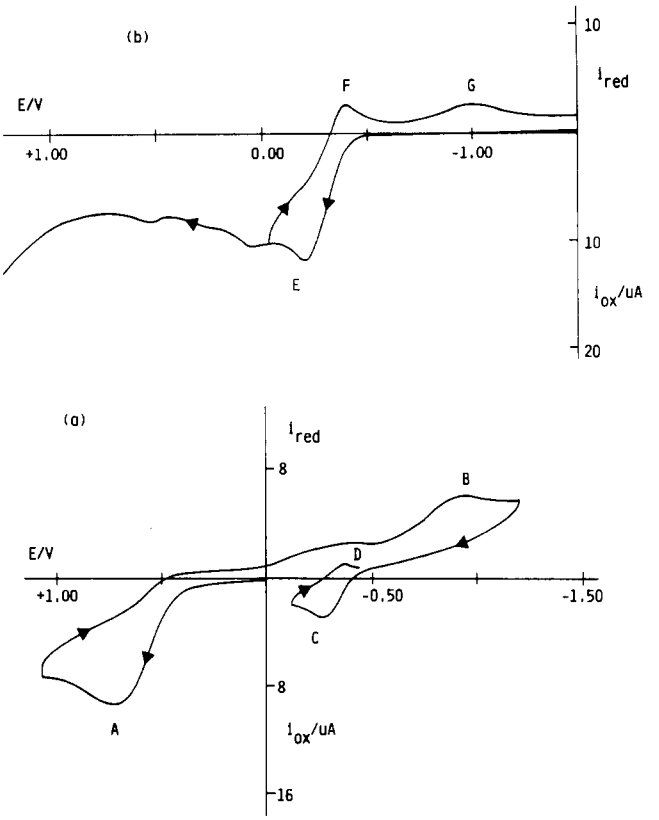

Figure 7. Cyclic voltammograms of deaerated THF solutions containing $[NBu_4]ClO_4$ (0.1 mol dm^{-3}) recorded at a platinum electrode: (a) complex **2** (1.30 × 10^{-3} mol dm^{-3}); (b) complex **12** (1.29 × 10^{-3} mol dm^{-3}). Scan rate = 0.2 V s^{-1}.

determination of the number of electrons involved in the oxidation process. However, a comparison with the one-electron oxidation of an equimolar solution of ferrocene indicates it to involve a one-electron step. The complex electrogenerated at peak A undergoes an irreversible reduction in correspondence to peak B (E_p = −0.94 V), generating a species which, in oxidation, gives rise to the peak system C/D ($E^{\circ\prime}$ = −0.31 V).

A comparison of the electron-transfer sequence with the cyclic voltammogram displayed by $[(PP_3)RhH]$ (**12**) (Figure 7b) provides useful information to gain insight into the redox behavior of **2**. The monohydrido complex undergoes an anodic oxidation at peak E that, in the reverse scan, displays an associated peak F as well as a further reduction at peak G. Analysis with scan rates[26] v, ranging from 0.02 to 2 V s^{-1} shows that (i) the $i_{p(F)}/i_{p(E)}$ ratio increases from 0.56 at 0.05 V s^{-1} to 1 at 2 V s^{-1}, (ii) the peak separation increases from 140 to 260 mV, and (iii) the $i_{p(E)}/\sqrt{v}$ ratio decreases by ca. 10%. All of these results are diagnostic of a quasireversible one-electron oxidation complicated by following chemical reactions. A rough evaluation of the lifetime of $[(PP_3)RhH]^+$ gives a value of $t_{1/2} \cong$ 3 s. The formal electrode potential for the couple $[(PP_3)RhH]^{+/0}$ is −0.31 V, coincident with that of the peak system C/D. In addition, peaks B and G are located at the same potentials (peak G is assigned to the reduction of the species that forms during the chemical complication following the one-electron removal). In view of all of these data, we reasonably conclude that the overall anodic process shown by **2** involves the deprotonation of the starting η^2-H_2 complex and an overall reaction path quite similar to that exhibited by the cobalt congener **1**.

$$[(PP_3)Rh(H_2)]^+ \xrightarrow[-H^+]{-e^-} [(PP_3)RhH]^+ \xrightarrow{t_{1/2} \cong 3s}$$

unidentified product

(22) (a) Geiger, W. E. *Prog. Inorg. Chem.* **1985**, *33*, 275. (b) Zanello, P. *Comments Inorg. Chem.* **1988**, *8*, 45.
(23) Ghilardi, C. A.; Sacconi, L. *Cryst. Struct. Commun.* **1975**, *4*, 149.
(24) Orlandini, A.; Sacconi, L. *Cryst. Struct. Commun.* **1975**, *4*, 157.
(25) Jahn, H. A.; Teller, E. *Proc. R. Soc. London, Ser. A* **1937**, *161*, 220.
(26) Brown, E. R.; Sandifer, J. R. In *Physical Methods of Chemistry. Electrochemical Methods*; Rossiter, B. W., Hamilton, J. F., Eds.; Wiley: New York, 1986; Vol. 2, Chapter 4.

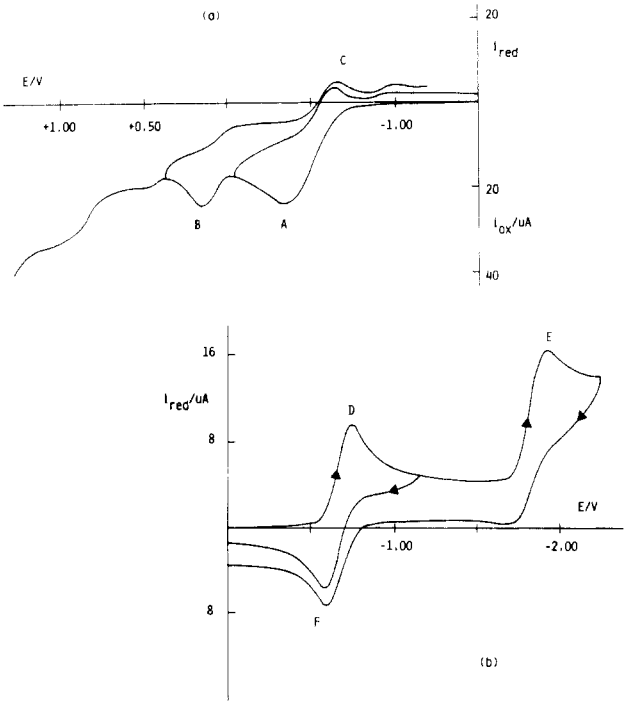

Figure 8. Cyclic voltammograms of deaerated THF solutions containing $[NBu_4]ClO_4$ (0.1 mol dm^{-3}) recorded at a platinum electrode: (a) complex **3** (1.81×10^{-3} mol dm^{-3}); (b) complex **5** (1.39×10^{-3} mol dm^{-3}). Conditions: argon atmosphere; scan rate 0.2 V s^{-1}.

Like the case of the cobalt complex **1**, no reduction process is observed for **2** within the potential range of THF.

$[(PP_3)Ir(H)_2]^+$, $[(NP_3)Rh(H)_2]^+$, and $[(NP_3)Ir(H)_2]^+$ vs $[(PP_3)M(H_2)]^+$ (M = Co, Rh). Unlike **1** and **2**, the classical dihydrides $[(PP_3)Ir(H)_2]BPh_4$ (**13**), $[(NP_3)Rh(H)_2]BPh_4$ (**14**), and $[(NP_3)Ir(H)_2]BPh_4$ (**15**) in THF show no redox activity in the potential range from −1.9 to +1.4 V.

$[(PP_3)Fe(H)_2]$ vs $[(PP_3)FeH]^+$. Figure 8 compares the cyclic voltammetric response exhibited by **3** (a) with that of **5** (b) in THF solution deareated with argon. Compound **3** undergoes a first anodic process at peak A coupled to a rereduction peak C and a second irreversible oxidation step at peak B.

Cyclic voltammograms at different scan rates of the peak system A/C show that the $i_{p(C)}/i_{p(A)}$ ratio increases progressively from 0.5 at 0.05 V s^{-1} to 0.8 at 1 V s^{-1} (at higher scan rates the voltammetric picture appears poorly defined because of the coalescence of the two oxidation steps). Contemporaneously, the ΔE_p term notably increases from 190 to 534 mV. Unfortunately, it was not possible to determine the number of electrons spent in such a redox change by controlled-potential coulometry because of a fast fall of the electrolysis current, likely due to electrode-poisoning phenomena. Nevertheless, a comparison with the one-electron oxidation of ferrocene makes plausible the assignment of the anodic steps to two distinct one-electron processes leading to the relatively unstable species $[(PP_3)Fe(H)_2]^+$ ($t_{1/2} \cong 3$ s, $E°'[(PP_3)Fe(H)_2]^+/[(PP_3)Fe(H)_2] = -0.48$ V) and to the completely unstable dication $[(PP_3)Fe(H)_2]^{2+}$ ($E_p = +0.015$ V), respectively.[27]

The iron(II) monohydrido complex **5** undergoes two subsequent reduction steps in correspondence to peaks D and E, the first one only displaying a directly associated response in the reverse scan, peak F (Figure 8b). Controlled-potential coulometry at −1.0 V indicates the consumption of one electron/molecule. The cyclic voltammogram recorded after exhaustive electrolysis is fully complementary to that reported in Figure 8b. These data suggest the stability of the Fe(I) species $[(PP_3)FeH]$ (**16**). Analysis of the cyclic voltammograms with scan rates confirm that the Fe(II)/Fe(I) reduction involves a simple quasireversible electron transfer (the $i_{p(F)}/i_{p(D)}$ ratio is constantly equal to unity, while ΔE_p progressively increases from 88 mV at 0.02 V s^{-1} to 145 mV at 2 V s^{-1}). The redox potential of the couple $[(PP_3)FeH]^+/[(PP_3)FeH]$ is located at −0.66 V. Also, Figure 8b shows that an irreversible Fe(I)/Fe(0) step is present at $E_p = -1.92$ V. In the anodic region, no Fe(II)/Fe(III) oxidation process was detected up to 1.5 V.

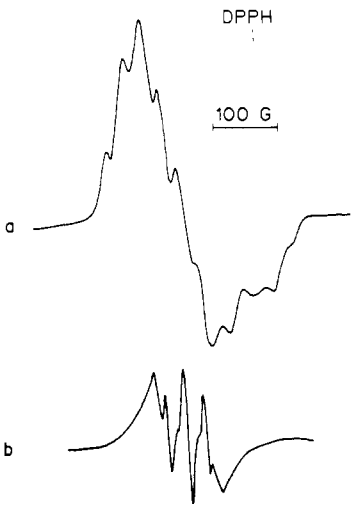

Figure 9. X-Band ESR spectra recorded on a THF solution of **5** under argon after its exhaustive one-electron reduction at $E_w = -1.0$ V: (a) T = 100 K; (b) T = 300 K.

A distorted TBP geometry can be assigned to the Fe(I) complex **16** on the basis of the X-band ESR spectrum in THF at 100 K (Figure 9a). This has been computed by using the following magnetic parameters: $g_1 = 2.110$ ($A_1 = 26.9$ G), $g_2 = 2.080$ ($A_2 = 10.0$ G), and $g_3 = 2.016$ ($A_3 = 34.9$ G). The coupling constants involving phosphorus have been introduced as mean values for the four nuclei. The spectrum at 300 K is shown in Figure 9b. One species only is present in ambient-temperature solutions with $\langle g \rangle = 2.068$ [$\langle A_P \rangle = 28.0$ G (2 P), $\langle A_P \rangle = 16.0$ G (2 P), $\Delta H = 15$ G]. Iron(I) complexes are exceedingly rare, and no hydride derivative has been so far reported.[28] The only complexes that appear closely related to **16** are the TBP Fe(I) σ-acetylides $[(PP_3)Fe(C{\equiv}CR)]$ obtained by reversible one-electron reduction of the Fe(II) derivatives $[(PP_3)Fe(C{\equiv}CR)]BPh_4$ (R = alkyl, aryl).[29] The latter compounds exhibit TBP structure, as authenticated by an X-ray analysis on the phenylacetylide congener $[(PP_3)Fe(C{\equiv}CPh)]BPh_4$. Since the fluid- and frozen-solution ESR spectra of **16** are quite similar to those of the Fe(I) acetylides $[(PP_3)Fe(C{\equiv}CR)]$, the former compound too is assigned TBP structure (Scheme II).

$[(PP_3)FeH(N_2)]^+$ vs $[(PP_3)Fe(H)(H_2)]^+$. In a previous paper we showed that the dihydrogen ligand in the *cis*-(hydride)(dihydrogen) complex **4** can be slowly displaced by dinitrogen to give $[(PP_3)Fe(H)(N_2)]BPh_4$ (**17**) (Scheme II).[2i] An electrochemical study in THF has been now carried out to determine the influence of H_2 vs N_2 on the redox properties of the two compounds. Complex **17** displays an irreversible oxidation process at E_p = +0.87 V, which tends to coalesce with the counteranion oxidation. Analogously, the dihydrogen derivative undergoes an irreversible oxidation at $E_p = +0.70$ V. Interestingly, both **4** and **17** undergo an irreversible reduction at $E_p = -1.1$ and −1.6 V through which the neutral dihydride **3** and the monohydride **16** are formed, respectively. As an example, we report the cyclic voltammetric response displayed by **4** in THF (Figure 10).

(27) Because of the instability of the compound, writing it as $[(PP_3)Fe(H)_2]^{2+}$ has no basis in observed fact. Indeed, this is an ideal compound to be formulated as an η^2-H_2 complex because it would then be d^6.

(28) Cotton, F. A.; Wilkinson, G. *Advanced Inorganic Chemistry*; Wiley: New York, 1988.

(29) Zanello, P.; Laschi, F.; Bianchini, C.; Peruzzini, M.; Proserpio, D. M.; Masi, D.; Mealli, C. *Abstracts*, XXVIIth ICCC, Brisbane, Australia, 1989; p W50.

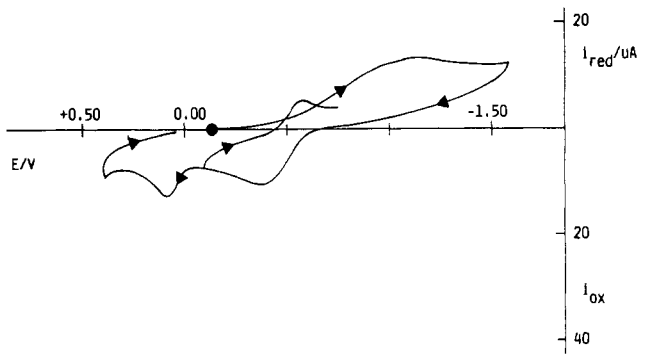

Figure 10. Cyclic voltammogram of a deaerated THF solution containing **4** (1.38×10^{-3} mol dm^{-3}) and $[NBu_4]ClO_4$ (0.1 mol dm^{-3}) recorded at a platinum electrode. Scan rate = 0.2 V s^{-1}.

Conclusions

Surveying the experimental evidence presented in this paper, one may readily infer that electrochemistry can provide a reliable, simple method to distinguish classical M-(H)$_2$ from nonclassical M-(H$_2$) structures within the numerous members of the $[(L)MH_2]^+$ family (L = PP_3, NP_3; M = Co, Rh, Ir). In fact, only those complexes, namely **1** and **2**, which exhibit the nonclassical structure, can be oxidized at potentials that are typical of monocationic d^8 metal complexes containing PP_3. Also, an electrochemical investigation has permitted us to eliminate any residual ambiguity concerning the controversial structure of the iron(II) dihydride **3**.

Further work is in progress to establish whether electrochemistry may really provide a diagnostic tool for dihydrogen binding. Very few comparative studies on the redox properties of dihydride/dihydrogen complexes have appeared in the literature, and some of them have produced conflicting results.[2r,30] In particular, Walton and Costello[30b] found electrochemical evidence for $ReH_7(PR_3)_2$ as being $Re(H_2)(H)_5(PR_3)_2$,[11c] but recent evidence indicates that the ReH_7 complexes are classical in both solid[31] and solution[13] states. Also, it is worth mentioning a recent work by Cotton and Luck, where the authors report the oxidation potentials in CH_2Cl_2 ($E_{1/2}$(ox) vs Ag/Ag$^+$) for $[ReCl_3(PMePh_2)_3]$ (0.9 V), $[ReCl(\eta^2\text{-}H_2)(PMePh_2)_4]$ (−0.07 V), $[ReH_3(PMePh_2)_4]$ (−0.17 V), and $[ReCl(CO)_3(PMePh_2)_2]$ (−0.17 V).[2r] Inspection of the $E_{1/2}$(ox) values revelas that the η^2-H_2 complex (formally Re(I)) is the easiest to oxidize whereas the trichloride (formally Re(III)) is the most difficult. Some ambiguity still surrounds the trihydride derivative, as it exhibits $E_{1/2}$(ox) and T_1 in the range of complexes possibly containing the dihydrogen ligand whereas an H-H separation of 1.96 (13) Å indicates a classical structure. On the other hand, the authors did not rule out the structure of an isomer containing only hydride ligands nor did they consider the possiblity that the complex might adopt a different structure in solution.[2n,4,31]

An important, original result presented in this paper concerns the deprotonation of the dihydrogen ligand upon oxidation of η^2 complexes. It is well-known that η^2-H_2 complexes can be deprotonated by either weak or strong bases, the acidity of the dihydrogen ligand depending on the relative degree of σ-donation to the metal and back-bonding from the metal into σ^* orbitals. However, by using a base, the deprotonation occurs through a direct attack at the η^2-H_2 ligand with no concomitant change of the metal oxidation state.[1,2c,q,32] Herein, we have shown that the deprotonation of the dihydrogen ligand can be achieved also by one-electron oxidation of η^2-H_2 complexes. As a result, a metal monohydride complex forms in which the formal oxidation state of the metal is now increased by 1 unit. This has allowed the synthesis of novel paramagnetic monohydrido complexes of cobalt and rhodium.

As a final consideration, we honestly doubt that the redox-induced deprotonation of the H_2 ligand may be a general reaction for dihydrogen compounds. In fact, **1** and **2** represent examples of η^2-H_2 coordination stabilized by d^8 L_4M fragments. In addition, an important role for the stabilization and chemistry of the dihydrogen ligand seems to be played by the unique bonding capabilities of the tripodal ligand PP_3.[3g] In actuality, most of the authenticated η^2-H_2 compounds belong to the d^6 L_5M family for which the oxidation of the metal may be more difficult to accomplish. As a matter of fact, no deprotonation of the dihydrogen ligand is observed for the Fe(II) complex **4** upon one-electron oxidation. In contrast, and this is another stimulating point, **4** converts to the neutral dihydride **3** upon one-electron reduction. We are presently studying this reaction, which is complicated by rapid intramolecular hydrogen exchange and the possible involvement of equilibrium concentrations of a trihydride species.[2i]

Experimental Section

General Data. All reactions and manipulations were routinely performed under a nitrogen or argon atmosphere with standard Schlenk tube techniques. The complexes $[(PP_3)Co(H_2)]PF_6$,[2j] $[(PP_3)Rh(H)_2]BF_4$,[4] $[(PP_3)Ir(H)_2]BPh_4$,[5] $[(NP_3)Rh(H)_2]BPh_4$,[6] $[(NP_3)Ir(H)_2]BPh_4$,[6] $[(PP_3)Fe(H)(H_2)]BPh_4$,[2i] $[(PP_3)Fe(H)(N_2)]BPh_4$,[2i,16] $[(PP_3)CoH]$,[7a] $[(NP_3)CoH]$,[7b] and $[(PP_3)RhH]$[6] were prepared as described in the literature. Ferrocenium hexafluorophosphate was prepared according to the literature method.[33] All the other chemicals were reagent grade and were used as received by commercial suppliers. Tetrahydrofuran, THF, was purified by distillation over $LiAlH_4$ under nitrogen just prior to use. Infrared spectra were recorded on a Perkin-Elmer 1600 Series FTIR spectrometer using samples mulled in Nujol between KBr plates. Proton NMR spectra were recorded at 299.945 MHz on a Varian VXR 300 spectrometer. The chemical shifts are reported relative to tetramethylsilane as external reference or calibrated against the solvent as the reference signal. $^{31}P\{^1H\}$ NMR spectra were recorded on a Varian VXR 300 spectrometer operating at 121.42 MHz. Chemical shifts are relative to external H_3PO_4 (85%) with downfield values reported as positive. The simulation of the $^{31}P\{^1H\}$ NMR spectra of the mixture of **3**, **3**-d_1, and **3**-d_2 was carried out by using a modified version of the DAVINS program.[14] The input data consisted of the experimental spectrum directly downloaded from the instrument. The simulation of the ^1H NMR resonances of the hydride ligands in **3** and **3**-d_1 was carried out by using an updated version of the LAOCN3 program.[34] The initial choices of shifts and coupling constants were refined by successive iterations, the assignment of the experimental lines being performed automatically. The final parameters gave a fit to the observed line positions better than 0.5 Hz. Conductivities were measured with a WTW Model LBR/B conductivity bridge. The conductivity data were obtained at sample concentrations of ca. 10^{-3} M in nitromethane solutions at room temperature. Magnetic susceptibilities of solid samples were measured on a Faraday balance. The materials and the apparatus used for the electrochemical experiments have been described elsewhere.[35] The potential values are relative to an aqueous calomel electrode (SCE) and refer to a controlled temperature of 20 ± 0.1 °C. Under the present experimental conditions, the ferrocenium/ferrocene couple was located at +0.56 V. The materials and the apparatus for recording the X-band ESR spectra have been described elsewhere.[36] The ESR spectra in fluid solutions were simulated by the computer program SL, which takes into account the line-width dependence on the m_i values for each group of equivalent nuclei.[37] The

(30) (a) Morris, R. H.; Earl, K. A.; Luck, R. L.; Lazarowych, N. J.; Sella, A. *Inorg. Chem.* **1987**, *26*, 2674. (b) Costello, M. T.; Walton, R. A. *Inorg. Chem.* **1988**, *27*, 2563.
(31) Howard, J. A. K.; Mason, S. A.; Johnson, O.; Diamond, I. C.; Crennell, S.; Keller, P. A. *J. Chem. Soc., Chem. Commun.* **1988**, 1502.
(32) (a) Crabtree, R. H.; Lavin, M.; Bonneviot, L. *J. Am. Chem. Soc.* **1986**, *108*, 4032. (b) Chinn, M. S.; Heinekey, D. M. *J. Am. Chem. Soc.* **1987**, *109*, 5865.
(33) Smart, J. C.; Piusky, B. L. *J. Am. Chem. Soc.* **1980**, *102*, 1009.
(34) Castellano, S.; Bothner-By, A. A. *J. Chem. Phys.* **1964**, *41*, 3863.
(35) Bianchini, C.; Mealli, C.; Meli, A.; Sabat, M.; Zanello, P. *J. Am. Chem. Soc.* **1987**, *109*, 185.
(36) Bianchini, C.; Laschi, F.; Mealli, C.; Meli, A.; Ottaviani, F. M.; Proserpio, D. M.; Sabat, M.; Zanello, P. *Inorg. Chem.* **1989**, *28*, 2552.
(37) (a) Ottaviani, M. F. *J. Phys. Chem.* **1987**, *91*, 779. (b) Romanelli, M. *J. Phys. Chem.* **1984**, *88*, 1663.

frozen-solution spectra were computed by using the program POWDER.[38]

Synthesis of the Complexes. The solid compounds were collected on sintered-glass frits and washed, unless otherwise stated, with ethanol and *n*-pentane before being dried in a stream of nitrogen.

Synthesis of $[(PP_3)Fe(H)_2]$ (3). Method A. $FeCl_2$ (0.05 g, 0.39 mmol) was added to PP_3 (0.27 g, 0.40 mmol) in 30 mL of THF, and the mixture was stirred for 10 min, producing a violet solution. $NaBH_4$ (0.1 g, 2.64 mmol) in 10 mL of ethanol was added and the mixture refluxed until an orange color appeared. By addition of ethanol (30 mL) and slow evaporation of the solvent in a stream of dinitrogen, yellow orange crystals of **3** precipitated (yield 80%). Anal. Calcd for $C_{42}H_{44}FeP_4$: C, 69.44; H, 6.10; Fe, 7.68. Found: C, 69.40; H, 6.02; Fe, 7.57.

Method B. To a stirred yellow solution of the (hydride)(η^2-dihydrogen) complex **4** (0.42 g, 0.40 mmol) in THF (30 mL) was added portionwise an equimolar amount of $KOBu^t$, and this mixture was stirred for 30 min. After $KBPh_4$ was filtered off, ethanol (25 mL) was added and the resulting solution evaporated in a stream of nitrogen until **3** precipitated in 70% yield.

Synthesis of $[(PP_3)FeH]BF_4$ (5). Method A. To a stirred suspension of **3** (0.36 g, 0.50 mmol) in ethyl ether (30 mL) was added dropwise an excess of $HBF_4 \cdot Et_2O$ until **3** completely dissolved while converting to violet, very hygroscopic microcrystals of **5**. These were filtered off and abundantly washed with dry ethyl ether (yield 90%). The compound can be carefully recrystallized from THF/ethyl ether. Anal. Calcd for $C_{42}H_{43}BF_4FeP_4$: C, 61.87; H, 5.31; Fe, 6.85. Found: C, 59.38; H, 5.49; Fe, 6.68.

Method B. Compound **4** (0.42 g, 0.40 mmol) was dissolved in a THF/EtOH mixture (4:1 v/v, 35 mL) under an argon atmosphere. On 2 h of bubbling with argon, the solution became deep violet and separated violet needles of **5** after addition of ethanol (30 mL); yield 80%.

(38) Courtesy of Prof. A. Bencini, Department of Chemistry, University of Firenze.

Synthesis of $[(PP_3)CoH]Y$. Y = BF_4 (7). Method A. $CoBF_4 \cdot 6H_2O$ (0.17 g, 0.50 mmol) in 5 mL ethanol was added to PP_3 (0.33 g, 0.50 mmol) in 30 mL of acetone, producing a brown solution. $NaBH_4$ (0.015 g, 0.40 mmol) in 10 mL of ethanol was slowly added and the mixture stirred until red-brown crystals of **7** precipitated (yield 85%). Anal. Calcd for $C_{42}H_{43}CoBF_4P_4$: C, 61.70; H, 5.30; Co, 7.21; P, 15.16. Found: C, 61.00; H, 5.17; Co, 7.28; P, 14.79.

Method B. To a yellow solution of **6** (0.36 g, 0.50 mmol) in 30 mL of THF was added solid $[(C_5H_5)_2Fe]PF_6$ (0.16 g, 0.50 mmol) with stirring. The solution immediately turned red-brown. A 10-fold excess of $[NBu_4)BF_4$ in ethanol (30 mL) was added and the solvent evaporated under a stream of nitrogen until crystals of **7** precipitated (yield 90%).

Safety Note. Perchlorate salts of metal complexes with organic ligands are potentially explosive. Only small amounts of material should be prepared, and these should be handled with great caution.

Y = ClO_4 (8). After exhaustive one-electron macroelectrolysis of **6** in THF at E_w = 0.0 V ($[NBu_4]ClO_4$ as supporting electrolyte), the solvent was fully evaporated. The crude product was washed three times with ethanol. The residue was collected and recrystallized from THF/*n*-heptane to give microcrystals of **8** (yield 75%). Anal. Calcd for $C_{42}H_{43}CoClO_4P_4$: C, 60.77; H, 5.22; Co, 7.10. Found: C, 60.52; H, 5.36; Co, 6.99.

Synthesis of $[(NP_3)CoH]ClO_4$ (11). After exhaustive one-electron macroelectrolysis of **9** in THF at E_w = -0.2 V ($[NBu_4]ClO_4$ as supporting electrolyte), the solvent was fully evaporated. The crude produce was washed three times with ethanol. The residue was collected and recrystallized from THF/*n*-heptane to give microcrystals of **11** (yield 40%). Anal. Calcd for $C_{42}H_{42}NCoClO_4P_3$: C, 62.04; H, 5.33; N, 1.72; Co, 7.44. Found: C, 61.12; H, 5.47; N, 1.63; Co, 7.21.

Acknowledgment. Part of this work was supported by the Progetto Finalizzato "Chimica Fine e Secondaria", CNR, Rome, Italy. Thanks are due to Mr. F. Zanobini for technical assistance.

Contribution from the Istituto per lo Studio della Stereochimica ed Energetica dei Composti di Coordinazione, CNR, Via J. Nardi 39, 50132 Firenze, Italy, Dipartimento di Chimica, Università di Siena, Via Pian dei Mantellini 441, 53100 Siena, Italy, and Dipartimento di Chimica Organica, Università di Firenze, 50121 Firenze, Italy

A Novel Oxygen-Carrying and Activating System of Rhodium(III). Oxidation and Oxygenation Reactions of 3,5-Di-*tert*-butylcatechol Catalyzed by a Rhodium(III) Cathecolate through Its (η^1-Superoxo)(η^2-semiquinonato)rhodium(III) Complex

Claudio Bianchini,*[†] Piero Frediani,[§] Franco Laschi,[‡] Andrea Meli,[†] Francesco Vizza,[†] and Piero Zanello[‡]

Received March 20, 1990

The coordinatively unsaturated Rh(III) catecholate complex [(triphos)Rh(3,5-DBCat)]$^+$ (2^+) has been synthesized by oxidative addition of 3,5-DBQ to the 16-electron fragment [(triphos)RhCl] [triphos = $MeC(CH_2PPh_2)_3$; 3,5-DBCat = 3,5-di-*tert*-butylcatecholate; 3,5-DBQ = 3,5-di-*tert*-butyl-*o*-benzoquinone]. Complex 2^+ undergoes electron-transfer reactions that encompass the Rh(III), Rh(II), and Rh(I) oxidation states of the metal and the catecholate, semiquinone, and quinone oxidation levels of the quinoid ligand. The Rh(II) derivative [(triphos)Rh(3,5-DBCat)] (3) and the Rh(III) semiquinone complex [(triphos)Rh(3,5-DBSQ)]$^{2+}$ (4^{2+}) have been characterized by X-band ESR spectroscopy [3,5-DBSQ = 3,5-di-*tert*-butylsemiquinonate]. Below 10 °C, complex 2^+ in CH_2Cl_2 or MeCN picks up dioxygen in a reversible manner, forming a diamagnetic dioxygen adduct, which has been identified by NMR and electrochemical techniques as [(triphos)Rh(η^1-O_2)(η^2-3,5-DBSQ)]$^+$ (5^+). The η^1-superoxo complex 5^+ is able to oxygenate inorganic substrates such as SO_2 and PPh_3 to sulfate and phosphine oxide, respectively. While the reaction with SO_2 is stoichiometric, leading to the stable η^2-sulfate-*O,O* complex [(triphos)Rh(SO_4)]$^+$, that with PPh_3 is catalytic under an oxygen atmosphere. The starting catecholate compound 2^+ is recovered intact after the catalysis cycle. 3,5-Di-*tert*-butylcatechol is both oxidized and oxygenated by 5^+ in a catalytic way producing *o*-quinone, muconic acid anhydride, and 2*H*-pyran-2-one. The oxidation to quinone, which is the prevailing reaction, is accompanied by production of H_2O_2. The characteristic features of the present nonenzymatic oxygenation of 3,5-di-*tert*-butylcatechol with molecular oxygen are as follows: (i) the process takes place in an intermolecular fashion, (ii) the catechol is oxygenated into the Hamilton intermediates of either the intra-diol or extra-diol type, and (iii) the oxygenation does not proceed through a quinone intermediate.

Due to its ability to accept as many as four electrons, dioxygen can react with transition metals, producing a great variety of oxo compounds.[1] However, in a preliminary stage, the interaction between O_2 and a metal system is a simple one, being practically limited to the formation of 1:1 adducts of either the superoxo or

Scheme I

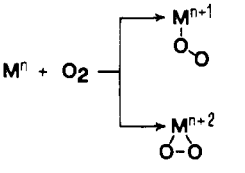

peroxo type (Scheme I). In both cases, the activation process requires an electron transfer from the metal to dioxygen. This

[†] ISSECC, CNR.
[‡] University of Siena.
[§] University of Florence.

0020-1669/90/1329-3402$02.50/0